ELSEVIER

Colloids and Surfaces
A: Physicochemical and Engineering Aspects 115 (1996) 55–62

COLLOIDS AND SURFACES A

Investigation of water in normal and dehydrated rabbit lenses by ^{1}H NMR and calorimetric measurements

Jerzy Bodurka [a,*], Gerd Buntkowsky [b], Robert Olechnowicz [a], Aleksander Gutsze [a], Hans-Heinrich Limbach [b]

[a] *Department of Biophysics, Medical School of Bydgoszcz, ul. Jagiellonska 13, 85-067 Bydgoszcz, Poland*
[b] *Institut für Organische Chemie der Freien Universität Berlin, Takustr. 3, D-14195 Berlin, Germany*

Received 12 September 1995; accepted 25 February 1996

Abstract

Water molecules in the lenses of animal eyes exist in two different states: water which is bound to proteins forming their hydration hull (nonfreezable) and free bulk water (freezable). Between these two types of water exchange processes take place on a time scale between approximately 10 and 100 ms, as has been shown by previous NMR relaxation studies of the lens. In this contribution we present results of experiments where we varied the relative amount of these two types of water by dehydration of the lens. The dehydration process removes primarily the free water from the lens. We monitored the changes of the relative fractions of water protons by measurements of the proton spin–lattice relaxation times and from the calorimetric curves of the eye lens. Both curves exhibit a strong singularity at the freezing point of the bulk water for the normal lens, which becomes smoother for increasing dehydration. To explain this effect on the spin–lattice relaxation time, a cross-relaxation process between bound water protons and protons in the frozen state must be assumed. From these experiments we were able to separate the individual relaxation times T_{1A} and T_{1B} of the two types of water, which are averaged out for the normal lens by the exchange process. We obtained also the activation parameters for free and bound water in the lens. We point out that the dynamic processes responsible for the water relaxation above the freezing point at 500 and 60 MHz are different. The relaxation data of the higher frequencies can be explained by assuming a fast motion (rotational diffusion of water molecules) with a single correlation time whereas for the lower frequencies additional type of molecular motions have to be taken into account.

Keywords: Dehydration; ^{1}H-nuclear magnetic resonance; Rabbit lens; Relaxation times; Water

1. Introduction

In recent years rapid progress in the clinical application of the magnetic resonance imaging (MRI) technique has been observed [1,2]. The magnetic spin–lattice (T_1) and the spin–spin (T_2) relaxation behaviour of the investigated samples are the principle image-forming mechanisms in MRI [3]. Therefore a quantitative understanding of the proton relaxation processes in biological systems is very important. Moreover since these relaxation processes depend in a characteristic way on the morphological and the pathological state of the tissues, a detailed understanding of proton relaxation processes in biological systems might yield valuable insights into these states. One such biological system is the mammalian lens. A normal mammalian lens contains about 65% of water and

* Corresponding author.

PII S0927-7757(96)03663-1

35% of organic material, mainly structural proteins. With this very high protein content (33% of the total weight), the lens has the highest protein concentration of all the organs in the body [4,5]. The fundamental function of the lens is to transmit and focus light reaching the eye onto the retina. A high degree of physiochemical order is needed to ensure transparency of the lens as has been shown by light scattering (in particular there exists a short range order of the lens proteins) [6,7]. The importance of the investigations of water behaviour in the lens results from the fact that through hydrophobic and hydrophilic interactions water contributes to the stabilisation of the three-dimensional macromolecular structures. Water in the lens is classified into freezable (free) and nonfreezable (bound, hydration) fractions [8–10]. The relative amounts of these two water fractions were established for the whole lens and its fragments for different species, from differential scanning calorimetry (DSC) and thermogravimetry analysis (TGA) [8,9]. Residual magnetic dipole interaction of water molecules in the lens cortex has been observed recently [11]. It was concluded that there is an anisotropic distribution of the water molecules or in other words the water is ordered. In this contribution we present T_1 measurements at 60 and 500 MHz resonance frequencies as a function of temperature together with calorimetric measurements for normal and dehydrated rabbit lenses to investigate the dynamical properties of water in the lens.

2. Material and methods

Measurements at 500 MHz were performed on whole lenses while at 60 MHz only parts of the lens could be measured. We used whole lenses ($n=3$) and parts from lenses ($n=3$), containing only material from the cortex, from two month old rabbits. The samples were used without any additional treatments. The experimental procedure was as follows: first the T_1 relaxation time as a function of temperature was measured for the whole lens (or cortex), then the dehydration process was carried out at room temperature on the same sample. These two steps were repeated three times for each sample. After partial dehydration of the lens, the NMR tube was sealed with a standard NMR rubber stopper to avoid further dehydration of the samples. The percentage of dehydration was determined by weighing the samples after each dehydration process. From this we calculated the dehydration degree as:

$$k_n = \frac{p_A p_D}{100\%} \tag{1}$$

where p_D is the percentage of dehydration, k_n is the dehydration degree and $k_n \in [0,p_A]$; n is the number of dehydrations ($n=0,1,2\ldots$); p_A is the fraction of free water protons (0.8 and 0.65 for the cortex and for the lens respectively [9]).

Sample dehydrations were done by using an SP500 (Unitra Unima, Poland) pump with pressure set to 10^{-1} hPa. Calorimetric measurements were done on the lens fragments containing material from cortex ($n=3$) using a home-built calorimeter as described earlier [12]. This device allows a precise determination of the crystallisation point of the lens as a function of various experimental parameters. The temperature of the lens was measured with a thermocouple and monitored as a function of time during the cooling or heating process. The cooling rate K_c and the heating rate K_h are experimental parameters which express the temperature change of the sample per unit time. The relaxation measurements at 60 MHz were done on a pulse NMR spectrometer (PMS-60, Radiopan, Poland). The spectrometer was equipped with a temperature control system, which allows stabilisation of the probe temperature to an accuracy of 0.5 K. Measurements at 500 MHz were performed on a Bruker AMX 500 spectrometer, which was equipped with a Bruker VT1000 temperature control unit. Absolute temperature accuracy was 1 K. Measurements of the spin–lattice relaxation time T_1 were performed in the temperature regimes from $25-30^{\circ}C$ at 500 MHz and from $21-50^{\circ}C$ at 60 MHz, because the denaturation of the lens proteins starts at $40^{\circ}C$ [4,5,7]. A typical 90° pulse width was 2.5 μs at 60 MHz and 10 μs at 500 MHz. The spin–lattice relaxation rates at 60 and 500 MHz were measured by the saturation recovery technique. At 60 MHz the relaxation rates

were determined from the intensity of the free induction decay after signal recovery and the relaxation functions obtained were analysed by a non-linear least squares method (Marquart algorithm) [13]. In all experiments a single exponential decay of the longitudinal relaxation function was observed. At 500 MHz we used the spectrum for calculating the relaxation rates. The analysis of the spectra established that there is a single, common T_1 value for the various line components [12].

3. Experimental results

Fig. 1 shows the results of the saturation recovery T_1 measurements, on a lens cortex (60 MHz), as a function of temperature for three different percentages of free water dehydration. Curves with 0% and 46% water dehydration show an increase in the relaxation time with increasing temperature

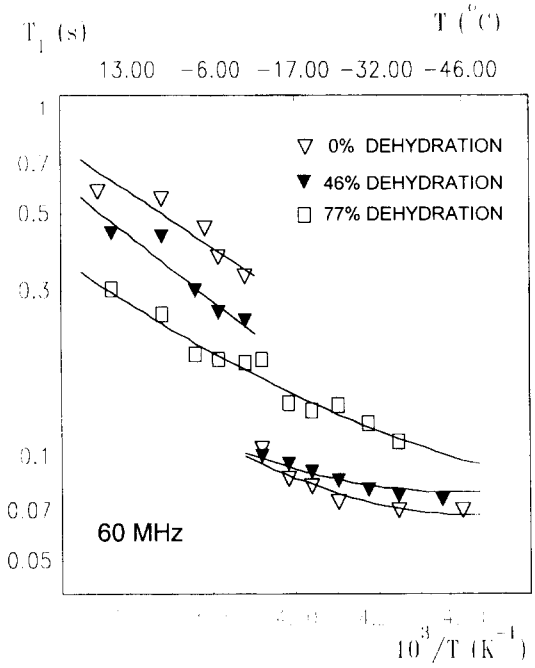

Fig. 1. The dependence of the spin–lattice relaxation time of the lens cortex for three different percentages of water dehydration (▽, 0%; ▼, 46%; □, 77%) on temperature measured at a Larmor frequency of 60 MHz. Solid lines result from fitting Eqs. (4)–(6) to the experimental data. The parameters of fitting are summarised in Table 1.

and a sudden step in the relaxation time at about −12 °C (261 K) which is caused by partial freezing of the lens water. The curve with 77% water dehydration is smooth over the whole temperature range. This shows that the dehydration process has removed almost all free water from the sample. Therefore the activation parameters obtained from that curve give information about the bound water dynamics (Table 1). At temperatures above the freezing point, increasing the percentage of dehydration decreases the spin–lattice relaxation time. An opposite tendency can be found below the freezing point where an increase in the percentage of dehydration leads to an increase in the relaxation time.

Fig. 2 shows the results of analogous experiments performed at 500 MHz. Curves with 0% and 25% dehydration show an increase in the relaxation time with increasing temperature and a sudden step in the relaxation time at about −8 °C (265 K) which is caused by partial freezing of the lens bulk water. The third curve at 59% dehydration indicates that the nonfreezable water fraction determines the overall spin–lattice relaxation rates, in the whole lens, because no discontinuity is observed. At temperatures above and below the freezing point the dependence of T_1 on the percentage of dehydration is similar to that at 60 MHz, namely decreasing and increasing of T_1 respectively.

The results of the calorimetric measurements on the rabbit lens cortex are shown in Figs. 3 and 4. Fig. 3 shows a typical example of the cooling–heating cycle with equal cooling and heating rates $K_c = K_h = 0.09$ K s^{-1}. As previously shown, undercooling of the lens is easy to achieve and the maximum undercooling temperature is an experimental parameter which can be adjusted by the cooling rate [12]. Therefore the different undercooling temperatures observed here are caused by the different cooling rates. Fig. 4 shows the set of cooling–heating cycles with the same cooling and heating rates obtained for the sample as a function of dehydration degree. It is evident that increasing the dehydration degree causes a decrease in the step observed in the cooling part of the cooling heating cycles. For the cycle labelled as D on Fig. 4, with the dehydration degree $k_3 = 0.72$ (which

Table 1
Results from fitting the T_1 curves with Eqs. (2)–(6) at different dehydration degrees, assuming a thermally activated Arrheuius process and the log-normal distribution of the correlation times. The fitting parameters are the activation energy (E_A); the correlation time for infinite temperature (τ_∞); the width (β) if the distribution of the correlation time.

Sample	Measurement frequency (MHz)	Above the freezing point			Below the freezing point		
		τ_∞ (s)	E_A (kJ mol^{-1})	β	τ_∞ (s)	E_A (kJ mol^{-1})	β
Cortex $k_0=0.0$	60	1.9×10^{-13}	12.1	1.2	9.7×10^{-13}	11.8	0.7
Cortex $k_1=0.36$	60	3.4×10^{-14}	16.6	1.1	1.3×10^{-13}	16.1	2.4
Cortex $k_1=0.62$	60	4.6×10^{-14}	15.6	2.3	4.6×10^{-14}	15.6	2.3
Cortex T_{1A}	60	3.2×10^{-14}	15.9	0.15	—	—	—
Whole lens $k_0=0.0$	500	9.7×10^{-15}	18.6	0.03	1.0×10^{-14}	20.5	0.03
Whole lens $k_2=0.17$	500	1.9×10^{-14}	17.4	0.05	4.0×10^{-15}	22.7	0.15
Whole lens $k_2=0.41$	500	7.1×10^{-15}	25.8	0.06	7.1×10^{-15}	25.8	0.06
Whole lens T_{1A}	500	2.9×10^{-14}	15.4	0.01	–	–	–

corresponds to 90% dehydration) the step in the curve has disappeared, therefore mainly the bound water fraction has remained in the sample. For different dehydration degrees the observed steps in the cooling–heating cycles correspond to the behaviour observed in the relaxation curves measured at 60 and 500 MHz (Figs. 1 and 2).

4. Discussion

To explain the spin relaxation properties of the water in the rabbit lens an exchange process between nonfreezable and bulk water was proposed [14–18]. Under the assumption that on the T_1 time scale fast water exchange among these water fractions takes place and that the dehydration process removes only water from the bulk state, the following theoretical expression can be obtained for the spin–lattice relaxation rate as a function of the dehydration degree k_n for temperatures above the freezing point:

$$\left(\frac{1}{T_1}\right)^{(n)} = \left(\frac{1}{T_{1B}}\right) + (k_n - p_A)\left(\frac{1}{T_{1B}} - \frac{1}{T_{1A}}\right) \qquad (2)$$

where T_{1v}, $v=$A,B, are longitudinal relaxation times for bulk and bound water protons; $(1/T_1)^{(n)}$ is the spin–lattice relaxation rate measured after n dehydrations.

The mobility of water molecules in the bulk phase is higher than in the bound phase. Thus one may expect that in general $T_{1A} > T_{1B}$ [14,16,17]. Therefore the above equation predicts that the observed spin–lattice relaxation rates should grow when increasing the dehydration degree. From Figs. 1 and 2 it can be seen that this is indeed observed. After the dehydration reaches 59% for the whole lens and 77% for the cortex, there are no further freezing effects in the T_1 curves. Therefore we may attribute these T_1 values to the bound water protons (T_{1B}, nonfreezable water). Using Eqn. (2) we may also separate the T_{1A} and T_{1B} values if we know any two values of the observed spin–lattice relaxation rates for two different dehydration degrees. On the other hand from T_{1B} the value of T_{1A} can be calculated at a given temperature. The results of such calculations are shown on Figs. 5 and 6 for 60 and 500 MHz respectively. The calculations were carried out for two different possible combinations of $T_1^{(n)}$ and

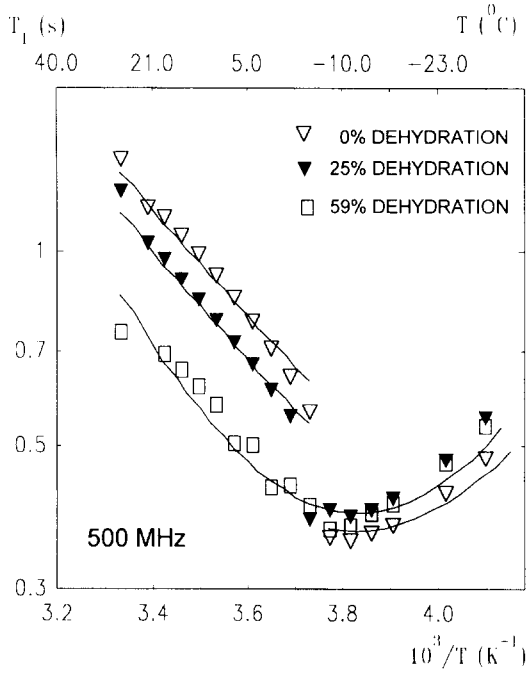

Fig. 2. The dependence of the spin–lattice relaxation time of the whole lens for three different percentages of water dehydration (▽, 0%; ▼, 25%; □, 59%) on temperature measured at a Larmor frequency of 500 MHz. Solid lines result from fitting Eqs. (4)–(6) to the experimental data. The parameters of fitting are summarised in Table 1.

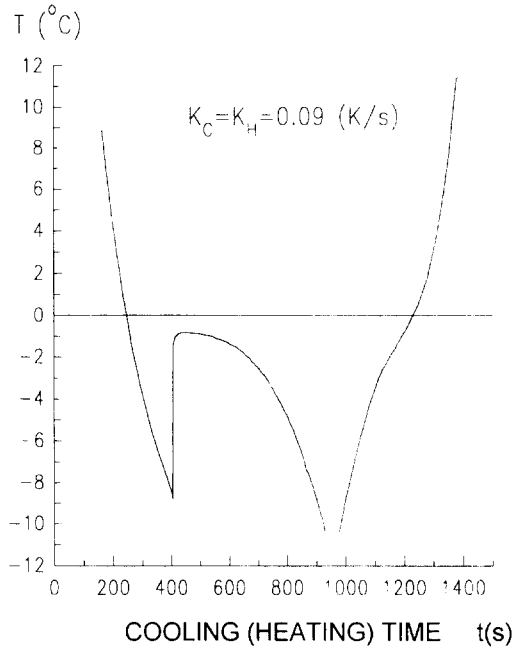

Fig. 3. A typical example of a calorimetric experiment on a fragment of the rabbit lens cortex. Shown are the temperature changes of the lens cortex during a cooling–heating cycle. The temperature of the sample was recorded as a function of the experimental time. The cooling and heating rates in the experiment were $K_C = K_H = 0.09$ K s^{-1}.

$T_1^{(k)}$ $(n \neq k = 0,1,2)$ and in each case the obtained values of T_{1A} and T_{1B} agree very well.

The observed step in $T_1^{(n)}$ for $n=0,1$ curves caused by the freezing process of the bulk lens water is most pronounced in the samples without dehydration ($n=0$), i.e. with the highest content of freezable water (Figs. 1 and 2). To explain this effect, cross-relaxation between bound water protons and protons in the frozen state was assumed. In the limit of rapid cross-relaxation, the expression for the observed T_{1F} spin–lattice relaxation is given by:

$$\frac{1}{T_{1F}} = \frac{p_B}{T_{1B}} + \frac{p_A}{T_{1L}} \tag{3}$$

where T_{1L} is the spin–lattice relaxation time of frozen water.

Comparing Eqs. (2) and (3) one obtains the conditions that $T_{1L} < T_{1A}$. It is known that spin–lattice relaxation times for hexagonal ice are much longer than calculated values of T_{1A} (Figs. 4 and 5) [19]. Furthermore it is also known that the internal motions in ice are strongly influenced by small amounts of impurities which may cause a reduction of T_{1L} of at least one order of magnitude [20]. The presence of proteins introduces structural defects. The frozen medium may be composed of ice slabs separated from proteins by a few molecular layers of bound, nonfrozen water. These water molecules provide a relaxation sink towards which the stored magnetic energy is transferred via cross-relaxation. The order of magnitude of T_{1L} values for the lens and for the cortex are of the same as in the case of clay gels [21].

Additionally we fitted all the relaxation data (solid line on figures), assuming that a thermally activated Arrhenius process is responsible for the relaxation curves (Eq. (4))

$$\tau_c = \tau_\infty \exp\left(\frac{E_A}{kT}\right) \tag{4}$$

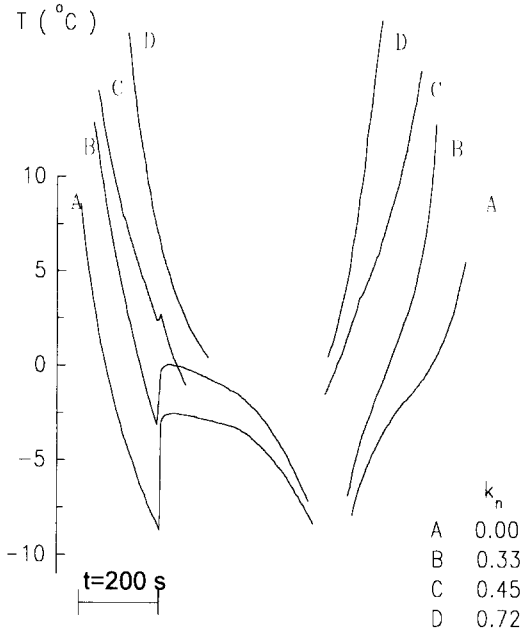

Fig. 4. Calorimetric results of the rabbit eye lens cortex fragment for four (A, $k_0=0.0$; B, $k_1=0.33$, C, $k_2=0.45$, D, $k_3=0.72$) different dehydration degrees (percentages of water dehydration, A, 0%; B, 41%; C, 56%; D, 90%). The cooling and heating rates were the same for all curves and equal to 0.12 K s^{-1}.

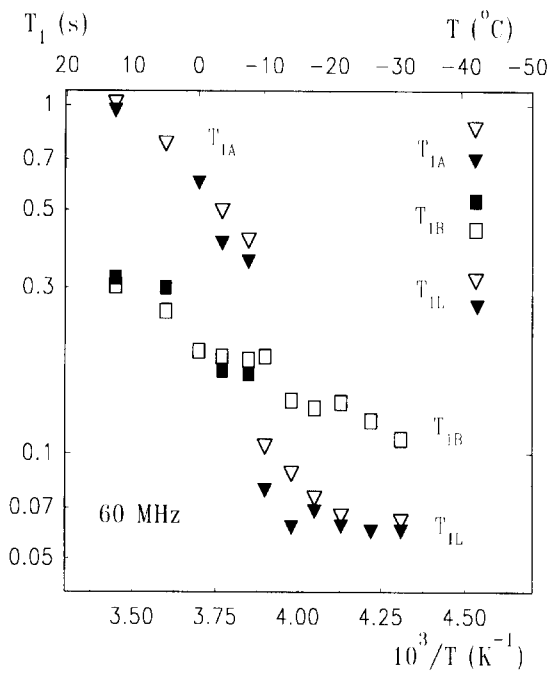

Fig. 5. The values of the spin–lattice relaxation times calculated from Eq. (2) for bound (T_{1B}; □, ■), free (T_{1A}; ▽, ▼) and frozen (T_{1L}; ▽, ▼) water. For calculations, two combinations of two different values of the observed spin–lattice relaxation times at 60 MHz ($T_1^{(v)}$; $T_1^{(p)}$ $v \neq p$ and $v,p=0,1,2$) were used.

where τ_∞ is the correlation time at infinite temperature and E_A is an activation energy expressed in kJ mol^{-1}.

Also a log-normal distribution of the correlation times given by Eqns. (4)–(6) [22] was assumed:

$$\frac{1}{T_1} = \int_0^\infty \frac{g(\tau_c)}{T_1(\tau_c)} d\tau_c \qquad (5)$$

where $g(\tau_c)$ is the normalised distribution function of the correlation times, and

$$f(s) = g(\tau_c)\frac{d\tau_c}{ds} = \frac{1}{\beta\sqrt{\pi}}\exp(s/\beta^2) \qquad (6)$$

where $s=\ln(\tau_c/\tau_0)$; τ_0 is the mean correlation time; β determines the width of the distribution.

The results of the fitting are summarised in Table 1. At high fields (resonance frequency 500 MHz) the distribution width is negligible, therefore it is sufficient to assume that the overall spin–lattice relaxation rate is due to fast molecular motion (i.e. the rotational diffusion of the water molecule) with a single correlation time. At low field (resonance frequency 60 MHz) it follows from the activation parameters obtained that the assumption of a single type of water motion with a single correlation time (or with a narrow distribution of correlation times) is not sufficient to explain the experimental data. At lower Larmor frequency, i.e. 60 MHz, the distribution widths are not negligible, but rather small which indicates that we have to take into account another type of molecular motion. To separate this other type of motion we used the activation parameters of the rotational motions obtained at 500 MHz to simulate the T_1 curves for other frequencies below the freezing point. The contribution to the spin–lattice relaxation rate of this other type of molecular motion should be lowest in this temperature range [20]. Therefore the deviation at low field gives evidence that rotational diffusion of water molecules is not sufficient to explain the observed spin–lattice relax-

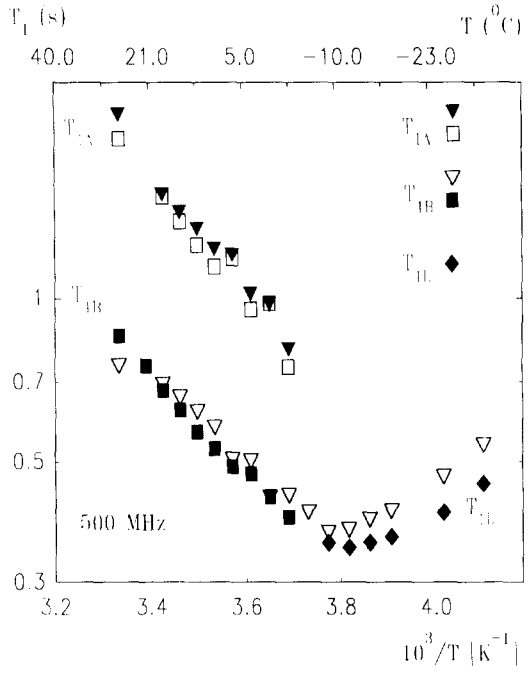

Fig. 6. The values of the spin–lattice relaxation times calculated from Eq. (2) for bound (T_{1B}; ▽, ■), free (T_{1A}; ▼, □) and frozen (T_{1L}; ◆) water. For calculations, two combinations of two different values of the observed spin–lattice relaxation times at 500 MHz ($T_1^{(v)}$; $T_1^{(p)}$ $v \neq p$ and $v,p = 0,1,2$) were used.

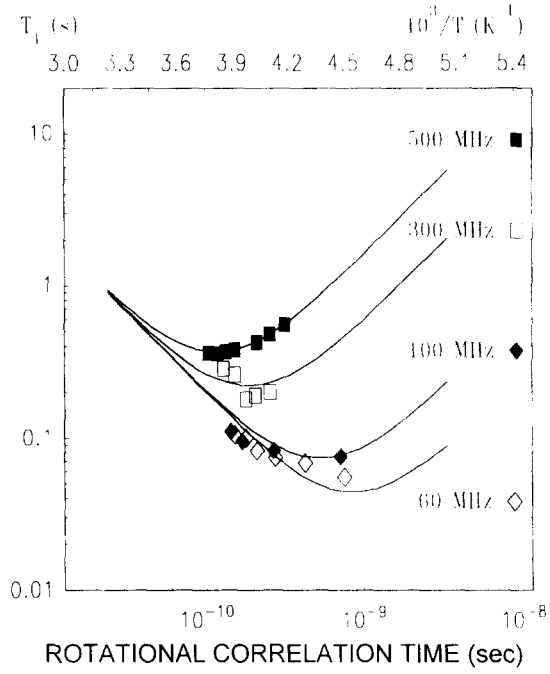

Fig. 7. The results of calculations from Eqs. (4)–(6) of the spin–lattice relaxation time as a function of temperature below the freezing point for 500 MHz (■), 300 MHz (□), 100 MHz (◆) and 60 MHz (◇), using the activation parameters obtained at the highest frequency (Table 1).

ation rate in the lens [20]. The results of these calculations are shown on Fig. 7. For the higher fields (500 and 300 MHz) the experimental data are reproduced very well whereas for the lower fields (100 and 60 MHz) deviations are found which are caused by the additional contribution to the overall relaxation rate. Additionally the big difference in the spin–lattice relaxation time measured in the lenses above freezing point at 60 and 500 MHz also indicates the presence of at least two different types of molecular motion that are responsible for the modulation of magnetic dipolar coupling of proton pairs. Therefore we postulate these results as further evidence for the anisotropic surface diffusion of water molecules proposed before [23–26].

5. Summary

In this work we investigated water dynamics in the rabbit lens by combining NMR relaxation measurements at two resonance frequencies with calorimetric measurements. Experiments were conducted on normal and dehydrated rabbit lenses. To interpret the experimental data the model of fast water exchange between bound and bulk water was used. The dehydration process allows us to control the relative fractions of bound and free water protons. A simple theoretical expression for the spin–lattice relaxation time T_1 as a function of the dehydration degree was derived which explains the experimental data well. We were able to separate spin–lattice relaxation times T_{1A} and T_{1B} characteristic of bulk and bound water respectively. The activation parameters for free and bound water in the lens were obtained. Additionally experimental evidence is given for the cross-relaxation effects between frozen and bound water. Finally we have shown that the dynamic processes responsible for the water relaxation at 500 and 60 MHz are different. In order to explain our relaxation data for the higher frequency the

assumption of fast motion (the rotational diffusion of water molecules) with a single correlation time is sufficient, whereas for lower frequencies an additional type of molecular motion has to be taken into account.

Acknowledgement

This work was supported by the KBN programme no. 4 P05A 015 10.

References

[1] R.E. Bushong, Magnetic Resonance Imaging: Physical and Biological Principles. Mosby, St. Louis MO, 1988.
[2] J.M.S. Hutchison, NMR proton imaging, in M.A. Foster (Ed.), Magnetic Resonance in Medicine and Biology, Pergamon Press, Oxford, 1985, pp. 157–212.
[3] P. Mansfield, P.G. Moris, NMR Imaging in Biomedicine, Academic Press, New York, 1982.
[4] H. Maisel, The Ocular Lens, Structure, Function, and Pathology, Marcel Dekker, New York, 1985.
[5] E. Cotlier, The lens, in A. Moses, (Ed.), Adler's Physiology of the Eye, Mosby, London, 1981, pp. 277–303.
[6] M. Delay and A. Tardieu, Nature, 302 (1983) 415.
[7] F.A. Bettelheim, Physical basis of lens transparency, in H. Maisel (Ed.), The Ocular Lens, Structure, Function, and Pathology, Marcel Dekker, New York, 1985, pp. 265–301.
[8] F.A. Bettelheim and N. Popdimitrova, Exp. "Eye" Res., 50 (1990) 715.
[9] I.-L. Cameron, E. Contreras, G.-D. Fulerton, M. Kellerman, A. Ludany and A. Miseta, J Cell. Physiol., 137 (1988) 125.
[10] F.A. Bettelheim, S. Ali, O. White and L.T. Chylak, Invest. Ophthalmol. Vis. Sci., 27 (1986) 122.
[11] J.A. Bodurka, A. Gutsze, G. Buntkowsky and H.-H. Limbach, Z. Phys. Chem., 190 (1995) 99.
[12] A. Gutsze, J. Bodurka, R. Olechnowicz, G. Buntkowsky and H.-H. Limbach. Z. Naturforschung, Teil C, 50 (1995) 410.
[13] P.R. Bevington, Data Reduction and Error Analysis for Physical Sciences, McGraw–Hill, New York, 1969.
[14] P.J. Stankiewicz, K.R. Metz, J.W. Sassani and R.W. Brigs, Invest. Ophthalmol. Vis. Sci., 30 (1989) 2361.
[15] M.C. Neville, C.A. Paterson, J.L. Rae and D. Woessner, Science, 184 (1974) 1072.
[16] S. Lerman, D.L. Ashley, R.C. Long, J.H. Goldstein, J.M. Megaw and K. Gardner, Invest. Opthalmol. Vis. Sci., 23(2) (1982) 218.
[17] A. Gutsze, J.A. Bodurka, R. Olechnowicz and A. Jesmianowicz, Colloids Surfaces A, 72 (1993) 295.
[18] P. Racz, K. Tompa and I. Pocsik, Exp. Eye Res., 29 (1979) 601.
[19] R. Blinc and H. Gränicher, Z. Phys. B, 22 (1975) 211.
[20] H.-W. Spiess, in P. Diehl, E. Auck and R. Kosfeld (Eds.), Rotation of molecules and nuclear spin relaxation, in Dynamic NMR Spectroscopy, Springer-Verlag, Berlin, 1978.
[21] J. Fripiat and M. Letellier, J. Magn. Reson., 57 (1984) 279.
[22] H. Pfeifer, in R. Kosfeld (Ed.), Nuclear magnetic resonance and relaxation of molecules adsorbed on solids, in NMR — Basic Principles and Progress, Vol. 7, Springer-Verlag, New York, (1972), pp. 55–153.
[23] G. Schauer, R. Kimmich and W. Nusser, Biophys. J., 53 (1988) 397.
[24] R. Kimmich, W. Nusser and T. Gneitting, Colloids Surfaces A 45 (1990) 283.
[25] R. Kimmich, F. Winter, W. Nusser and K.-H. Spohn, J. Magn. Reson., 68 (1986) 263.
[26] J. Bodurka, G. Buntkowsky, A. Gutsze and H.-H. Limbach, Z. Naturforschung, 51C (1990) 81.